

N74-14595

## TRANSIENT ANALYSIS USING CONICAL SHELL ELEMENTS

By Jackson C. S. Yang, Jack E. Goeller,  
and William T. Messick

Naval Ordnance Laboratory

### SUMMARY

The use of the NASTRAN conical shell element in static, eigenvalue, and direct transient analyses is demonstrated. The results of a NASTRAN static solution of an externally pressurized ring-stiffened cylinder agree well with a theoretical discontinuity analysis. Good agreement is also obtained between the NASTRAN direct transient response of a uniform cylinder to a dynamic end load and one-dimensional solutions obtained using a method of characteristics stress wave code and a standing wave solution. Finally, a NASTRAN eigenvalue analysis is performed on a hydroballistic model idealized with conical shell elements.

### INTRODUCTION

One of the principal areas of interest at the Naval Ordnance Laboratory is high-speed water entry of naval ordnance. In order to achieve stable water entry (no broaching) at low entry angles off the horizontal, the nose is frequently made blunt so that the impact force is nearly axial. The rise time of the impact force can be quite small, depending on the entry angle. Hence, a transient analysis of structural response is required. This paper deals with an analysis of a ring-stiffened hydroballistic model which is designed to impact the water at very high speeds. The NASTRAN conical shell element appeared to be useful since many of the models tested at NOL are axisymmetric, monocoque structures of contour shape which are exposed to external pressure and axial and transverse loads. However, there has been little reported use of this element. Reference 1 illustrates its use in a modal analysis of a ring-stiffened shell and demonstration problem 1.5 (reference 2) is a static loading of a uniform cylindrical shell. In order to gain confidence in the use of the conical shell element before modeling the hydroballistic model, simple structures were analyzed and the results compared to theoretical values. NASTRAN runs were made on the CDC 6400 computer at NOL using Level 15.1.1.

## SYMBOLS

A	cross-sectional area of shell
E	modulus of elasticity
$F_0$	constant end load on cylindrical shell
h	thickness of cylindrical shell
L	length of cylindrical shell
m	mass per unit length of cylindrical shell
$M_x$	axial moment per unit length
R	radius of neutral axis of circular cylinder
t	time
'	rise time of force pulse
u	axial displacement
x	axial distance
$\delta$	displacement of circular shell at junction with ring stiffener
$\nu$	Poisson's ratio
$\sigma_\phi$	hoop stress
$\sigma_x$	axial stress
$\omega_r$	rth eigenvalue in circular frequency

## EXTERNALLY PRESSURIZED RING-STIFFENED CYLINDER

The ring-stiffened shell section of a hydroballistic model was analyzed to determine the stresses when it is exposed to external pressure during launch in the gas gun. A midsection consisting of three typical bays was analyzed. The shell was assumed to be clamped at each end (no pressure applied at ends). Figure 1 depicts the finite elements used in synthesizing the NASTRAN model of the ring-stiffened cylindrical shell. The overall model had 96 rings (or grid circles) and 95 elements, yielding a total of 471 degrees of freedom for each harmonic.

The zeroth harmonic was used in the problem since the loading was axisymmetric. The material for the model is aluminum. Element forces, bending moments, stresses and ring point deflections were obtained for an externally applied pressure load of  $6.894 (10^6) \text{ N/M}^2$ . To gain further insight in using conical shell elements, multipoint constraints were applied to the ring at the junction between the ring stiffener and the cylindrical shell. This eliminates the overlapping of material from the stiffener and the cylindrical shell, see Figure 1. The number of elements was also varied to observe the effect of element size.

A discontinuity analysis was done on the ring-stiffened cylinder in order to assess the accuracy of the NASTRAN results. The rings were considered to have a thick-walled Lamé stress distribution caused by the discontinuity shear force at the ring-shell junction. The short shell between rings was considered a beam on an elastic foundation so that displacement and slope relations from reference 3 were used. By using compatibility of slopes and displacements at the junction, the discontinuity shear and bending moment were obtained. Axial and hoop stresses were calculated from

$$\sigma_x = \pm \frac{6M_x}{h^2}$$

$$\sigma_\phi = \frac{E\delta}{R} \pm \nu \frac{6M_x}{h^2}$$

The significant results from the NASTRAN static analysis (rigid format one) and the discontinuity analysis are presented in Figures 2 through 5. Figure 2 shows a comparison of the radial displacement along the center bay. Figure 3 shows the hoop stress at the inside and outside wall. The agreement is quite good. Figures 4 and 5 show the comparison of the axial bending moment and axial stress. The agreement is quite good in close proximity to the stiffener, but gradually deviates near the midspan of the bay. This might possibly be improved by using smaller elements. The ring size was very important around the stiffeners because of the rapid attenuation of the bending moment. Very few differences were observed when MPC was used at the junctions of the shell and the stiffeners. This indicates that the overlapping does not have too much effect on the results for the shell-to-ring thickness ratio used in this problem.

## RESPONSE OF UNIFORM CYLINDER TO DYNAMIC AXIAL LOAD

In a typical water-entry body, the structure is exposed to transient loading and the body must be considered as free-free. Before proceeding to actual modeling of the complex structure involving stiffening rings, etc., several simplified structural models were investigated and comparisons made with known classical solutions. Rigid format nine, "direct transient analysis," was used in the NASTRAN program. Figure 6 depicts the finite elements used in synthesizing the NASTRAN model of the cylindrical shell. The overall model had 21 rings (or grid circles) and 20 elements, yielding a total of 42 degrees of freedom for each harmonic. The zeroth harmonic was used in the problem since the loading was axisymmetric.

The transient dynamic stresses, element forces, and deflections were obtained for selected elements and rings. Three cases of dynamic loads were applied to one end of the cylindrical shell. The dynamic loads consist of a constant force with two different rise times and a trapezoidal pulse. These dynamic loads are specified on TABLED1, TLOAD1, and DAREA cards. The structure was considered as having free-free boundary conditions. Comparisons of the NASTRAN results were made with one-dimensional stress wave code which uses the method of characteristics and also a one-dimensional closed form standing wave solution. These latter solutions do not include the effect of hoop stress as the NASTRAN element does.

The standing wave solution was obtained for a free-free bar loaded at the end  $x = 0$ , by a force which is a ramp to time  $t_0$  and a constant  $F_0$  after  $t_0$ . The displacement of the bar is given by (see reference 4)

$$0 \leq t \leq t_0$$

$$u(x,t) = \frac{F_0}{mLt_0} \frac{t^3}{6} + \frac{F_0}{EAL} \left( \frac{t}{t_0} \right) \left[ \frac{(L-x)^2}{2} - \frac{1}{6} L^2 \right]$$

$$- \frac{2F_0}{mLt_0} \sum_{r=1}^{\infty} \frac{\sin \omega_r t}{\omega_r^3} \cos \left( \frac{r\pi x}{L} \right)$$

$$t_0 \leq t$$

$$u(x,t) = \frac{F_0}{mL} \left[ \frac{t_0^2}{6} + \frac{t^2}{2} - \frac{t_0 t}{2} \right] + \frac{F_0}{EAL} \left[ \frac{(L-x)^2}{2} - \frac{1}{6} L^2 \right]$$

$$- \frac{2F_0}{mL^2} \sum_{r=1}^{\infty} \frac{\sin \omega_r t - \sin \omega_r (t-t_0)}{\omega_r^3} \cos \left( \frac{r\pi x}{L} \right)$$

$$\text{where } \omega_r = r\pi \sqrt{\frac{EA}{mL^2}}$$

The first term is the rigid body motion. The second term may be looked upon as the static deformation; the series represents the harmonic oscillation terms. The stress can be computed from

$$\sigma_x = E \frac{\partial u}{\partial x}$$

Figure 7 shows a comparison of displacement at the end ( $x = 0$ ) where the force is applied and at the midspan ( $x = 152.4$  cm). The NASTRAN solution follows the simplified theoretical solution reasonably well. Figure 8 shows a comparison of the axial stress at the neutral axis of the first element and the midspan element. This axial stress was used since the theoretical solution ignores bending stress. The comparisons are, in general, not bad. There appears to be some long-time effect, but this might be due to the rather large element size used in the NASTRAN solution. Figures 9 and 10 show similar comparisons, except a shorter rise time was used on the loading functions. Figure 11 shows a comparison of axial stress at the first element and midspan element for a trapezoidal loading pulse. Again, the comparison with the one-dimensional stress wave theory is reasonably good.

#### EIGENVALUE ANALYSIS OF HYDROBALLISTIC MODEL

The hydroballistic model and the finite element discretization are shown in Figure 12. The length of the model is 345.12 cm and the body diameter is 34.29 cm. It consists of a thick-walled titanium nose section and ring-stiffened aluminum mid and tail sections. The aluminum skin is .794 cm thick. Four equally spaced fins are attached to the midsection and four to the tail section.

The blunt nose of the model causes the load at water impact to be nearly axial. Therefore, the axial mode of vibration of the model was examined. Figure 12 shows the 74 rings and 74 conical shell elements used to represent the model. The neutral axis of some of the elements has been moved instead of retaining the original positions and using MPC's to connect the rings.

The reason is that in a static analysis of a clamp band which had MPC'd rings at discontinuities in section, an ill-conditioned stiffness matrix was obtained. The "epsilon sub E" check yielded values on the order of one. Since the changes in stiffness of the hydroballistic model sections were even more severe, it was thought that for a first solution, a slight loss in accuracy from modifying the model would be acceptable.

The eigenvalue analysis was performed for axial vibration by allowing radial and axial displacement and axial rotations at each ring. Thus, a 222-degree-of-freedom model was analyzed. The first ten modes of vibration are given in Table 1. The fundamental mode of 282 cycles per second seems reasonable. Shifting the neutral axes of some shell sections yielded a well-conditioned matrix with the "epsilon sub E" check having a value of  $3 \times 10^{-13}$ .

The transient response to an axial impulse will be obtained and the results compared to the data obtained from the instrumented hydroballistic model with a water-entry velocity of 305 meters per second.

#### CONCLUSIONS

The results obtained from using the NASTRAN conical shell element agree well with theory. Using a 90-degree orientation for the conical shell element and an MPC for representing a ring stiffener yields excellent results. However, using MPC's to connect discontinuities in neutral axis radii can lead to ill-conditioned matrices.

Using the conical shell element in static analyses is routine. However, in the process of applying rigid format nine (direct transient analysis) to conical elements, a number of non-standard procedures must be practiced in order to obtain the results. The P field in the DAREA bulk data card must be determined by the following formula:

$$P = \text{ring ID} + 10^6 * (\text{Harmonic} + 1)$$

In the case control deck, reference to "grid points" is by the same formula. In the executive control deck, an alter must be used to switch to Sort 1 output. This enables the output to be printed in an orderly fashion.

It is hoped that some of the bugs encountered in using the conical shell element will be eliminated so that more use can be made of it. For axisymmetric structures subjected to loads which may be accurately expressed with a small number of

harmonics, it is less costly to use this element than to model with a large number of plates.

#### ACKNOWLEDGEMENTS

The authors would like to thank Dr. G. Everstine of the Naval Ship Research and Development Center and Mr. R. Edwards of the Naval Ordnance Laboratory for their helpful assistance and suggestions.

#### REFERENCES

1. Everstine, G., Ring-Stiffened Cylinder, Proceedings of the NSRDC-NASTRAN Colloquium, held at NSRDC, Washington, D. C., 12-13 Jan 1970, Paper 3.3
2. NASTRAN Demonstration Problem Manual (Level 15), NASA SP-224(01), Jun 1972
3. Hetényi, M., Beams on Elastic Foundation, The University of Michigan Press, Ann Arbor, Michigan, 1967
4. Meirovitch, Leonard, Analytical Methods in Vibrations, Macmillan Company, New York, New York, 1967

Table 1 - Eigenvalues for the Hydroballistic Model

Mode Number	Eigenvalue (cycles/second)
1	0.0
2	282
3	644
4	843
5	1365
6	1692
7	2300
8	2582
9	2975
10	3194

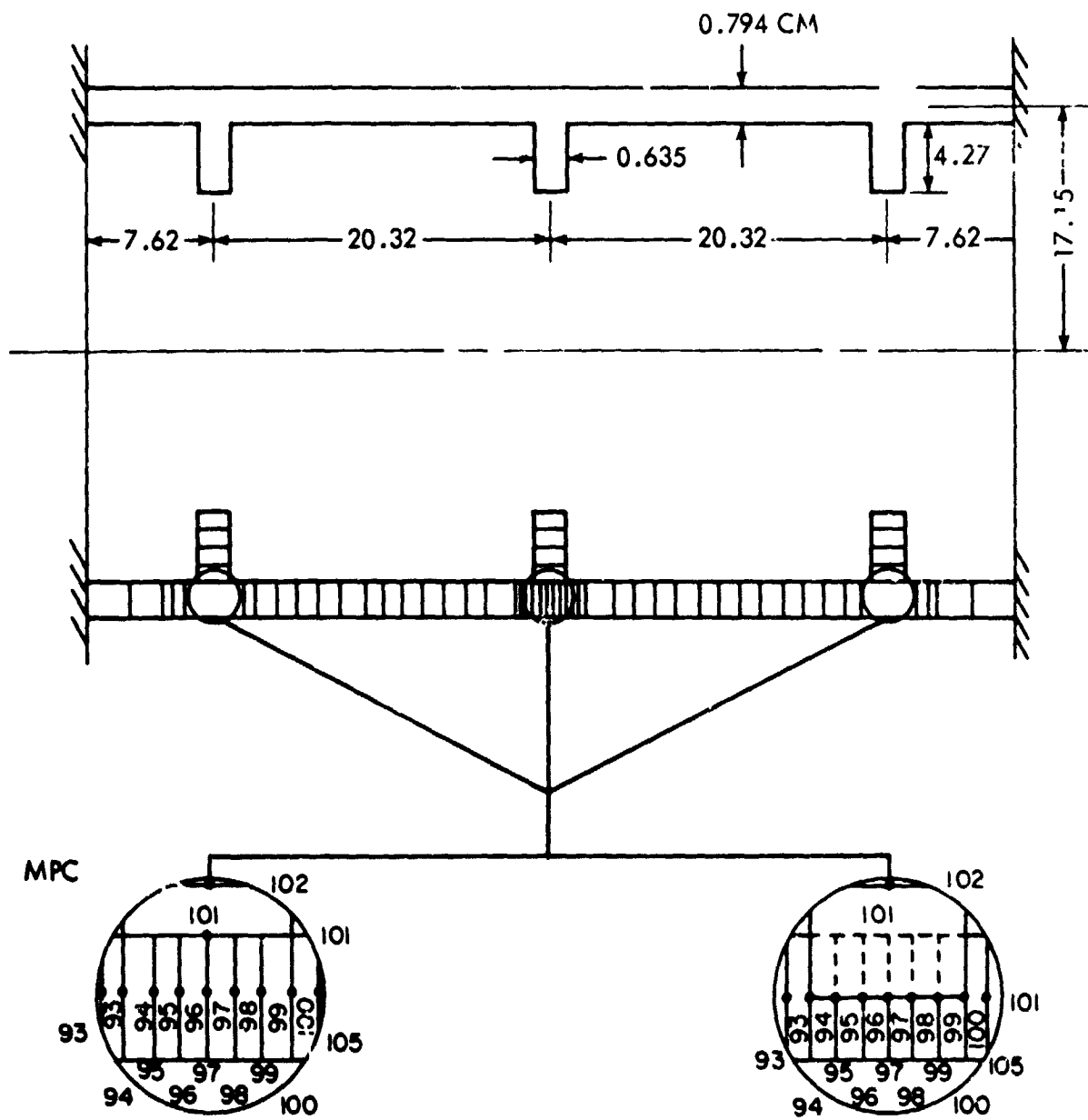


FIGURE 1 NASTRAN MODEL OF EXTERNALLY PRESSURIZED RING-STIFFENED SHELL

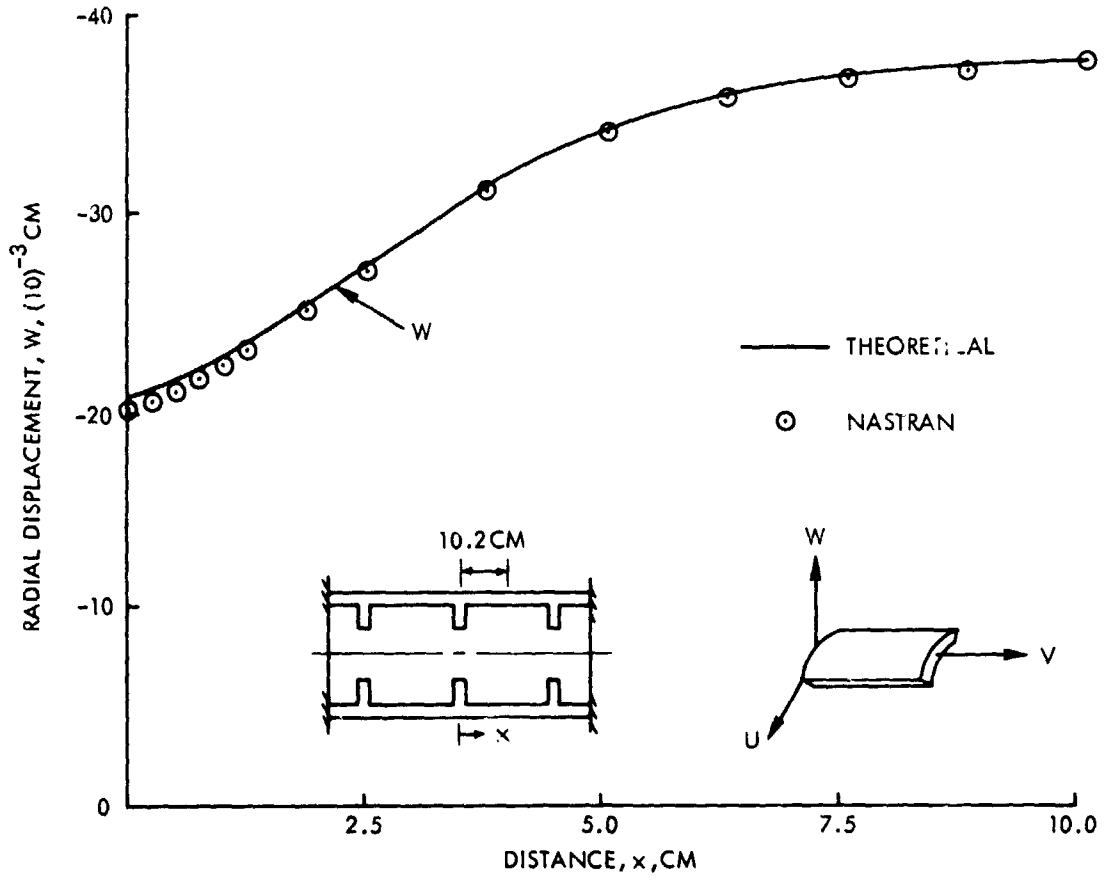


FIGURE 2 RADIAL DISPLACEMENT

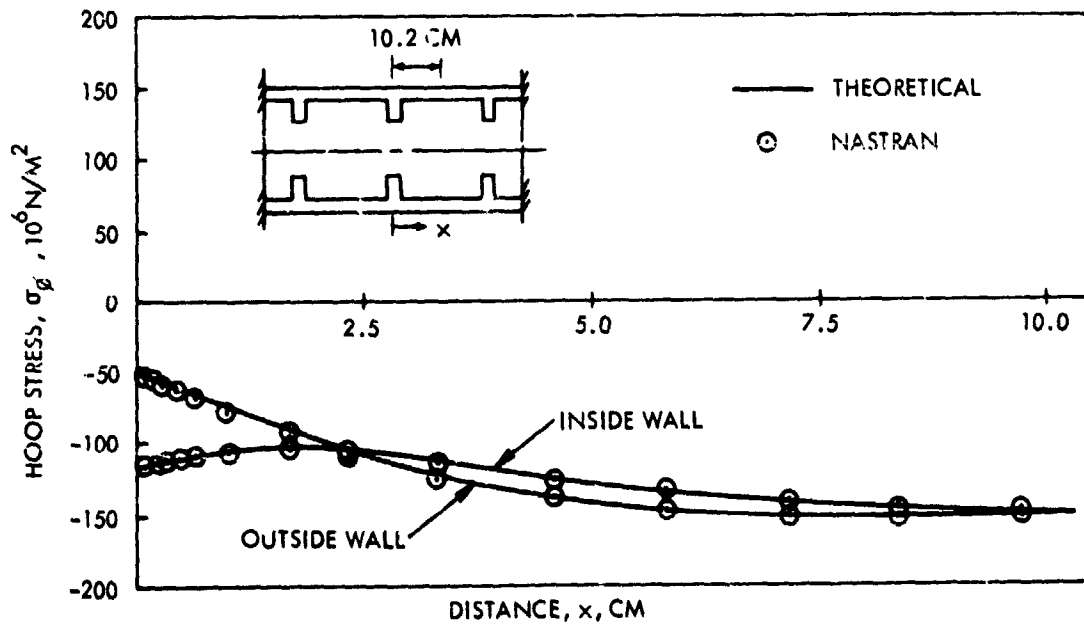


FIGURE 3 HOOP STRESS

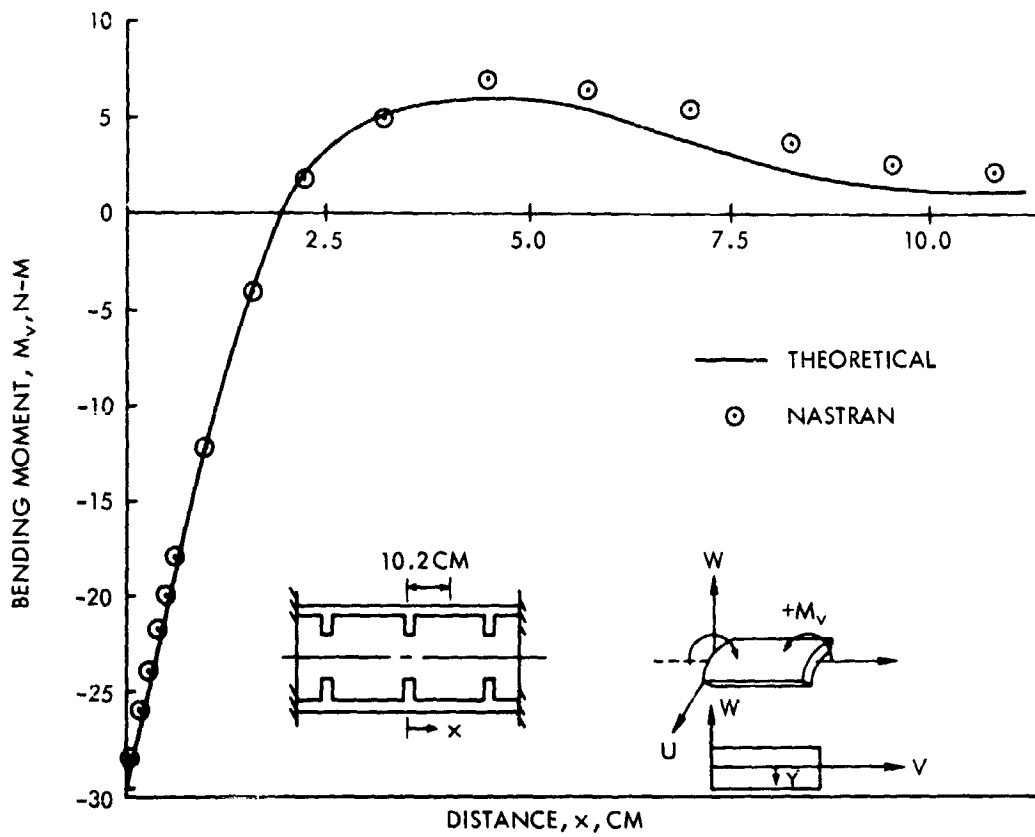


FIGURE 4 AXIAL BENDING MOMENT

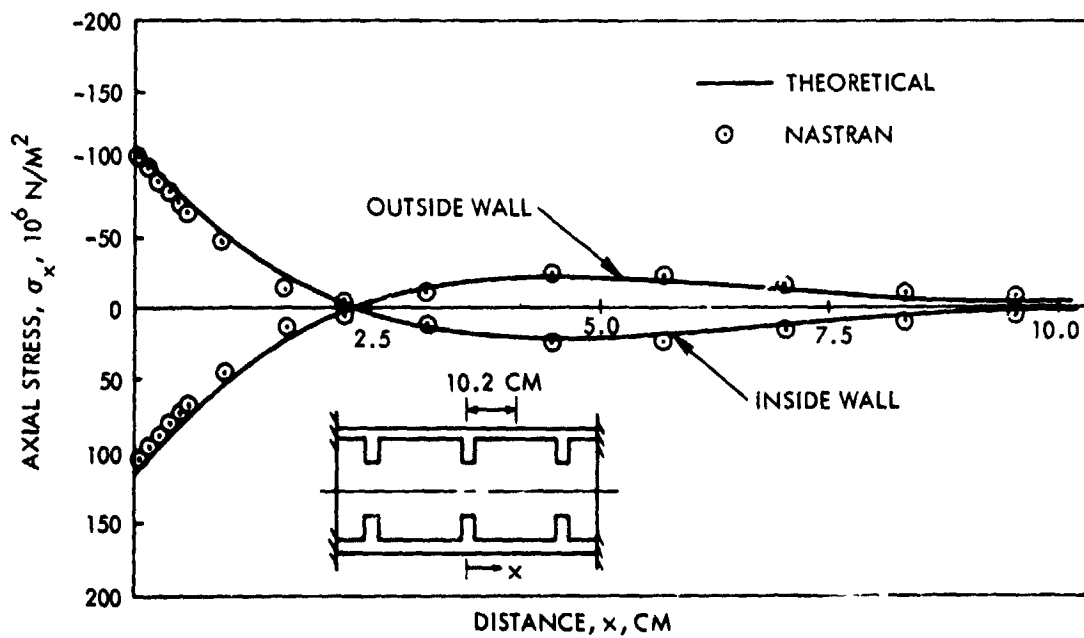


FIGURE 5 AXIAL STRESS

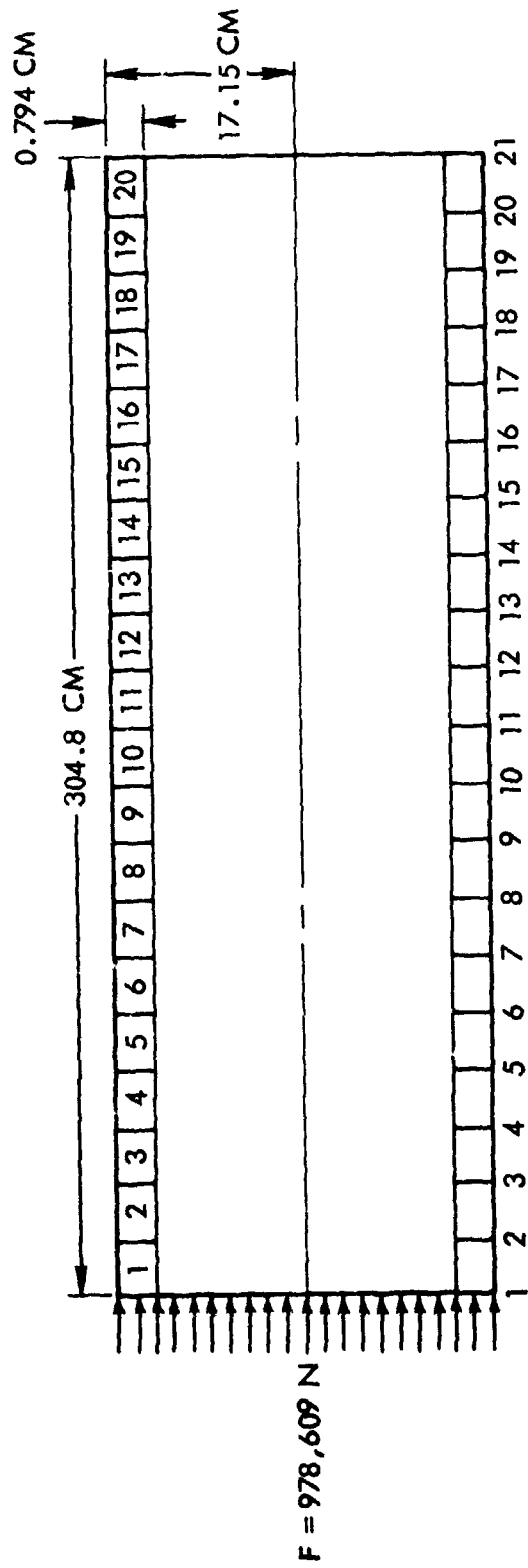


FIGURE 6 NASTRAN MODEL OF END-LOADED CYLINDER

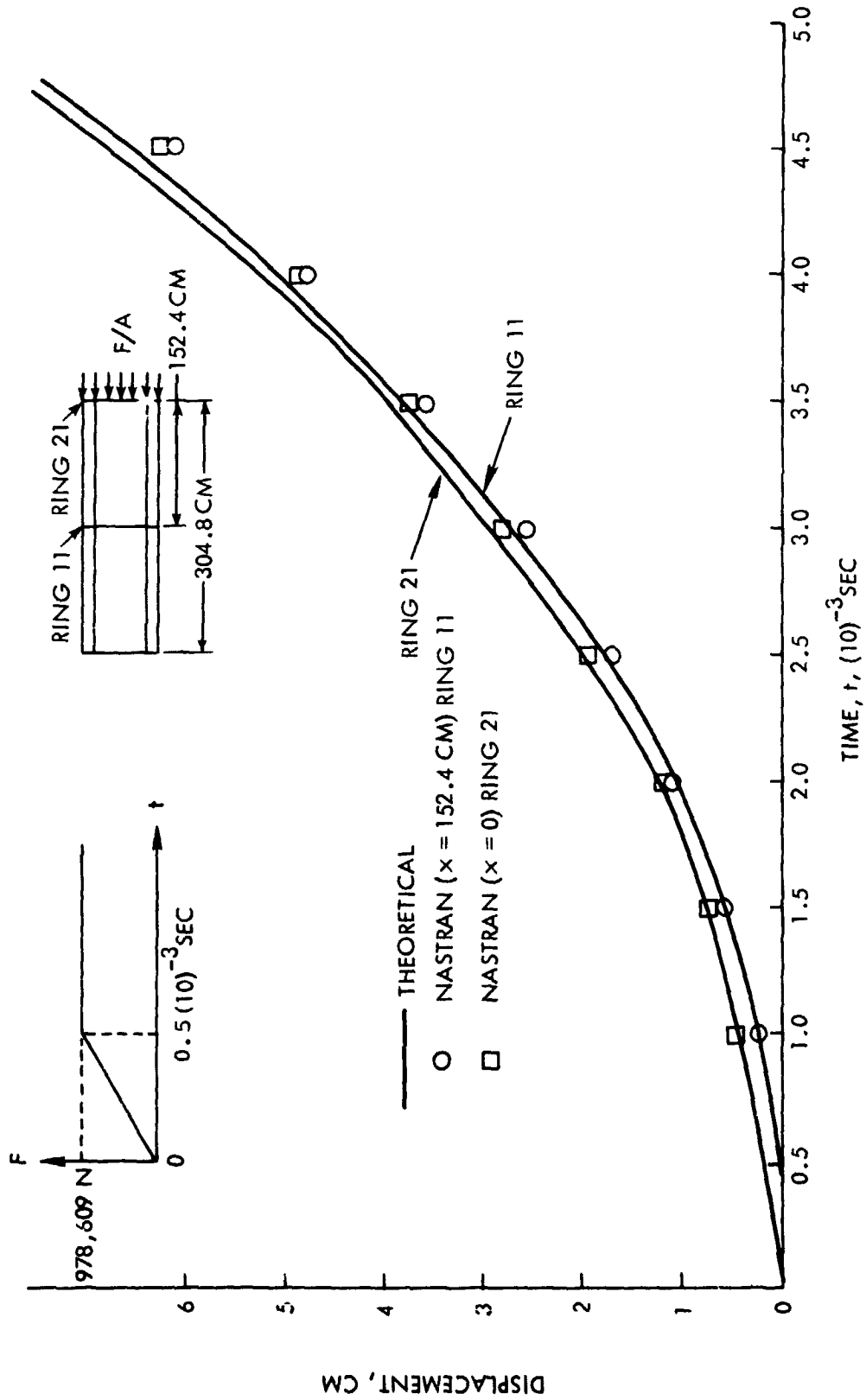


FIGURE 7 AXIAL DISPLACEMENT

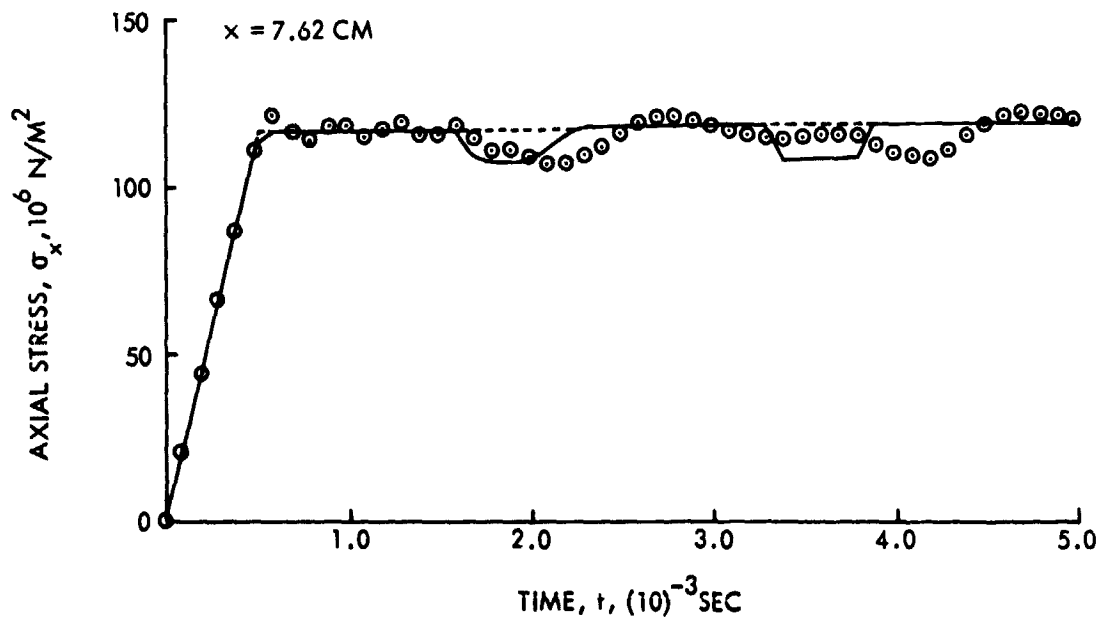
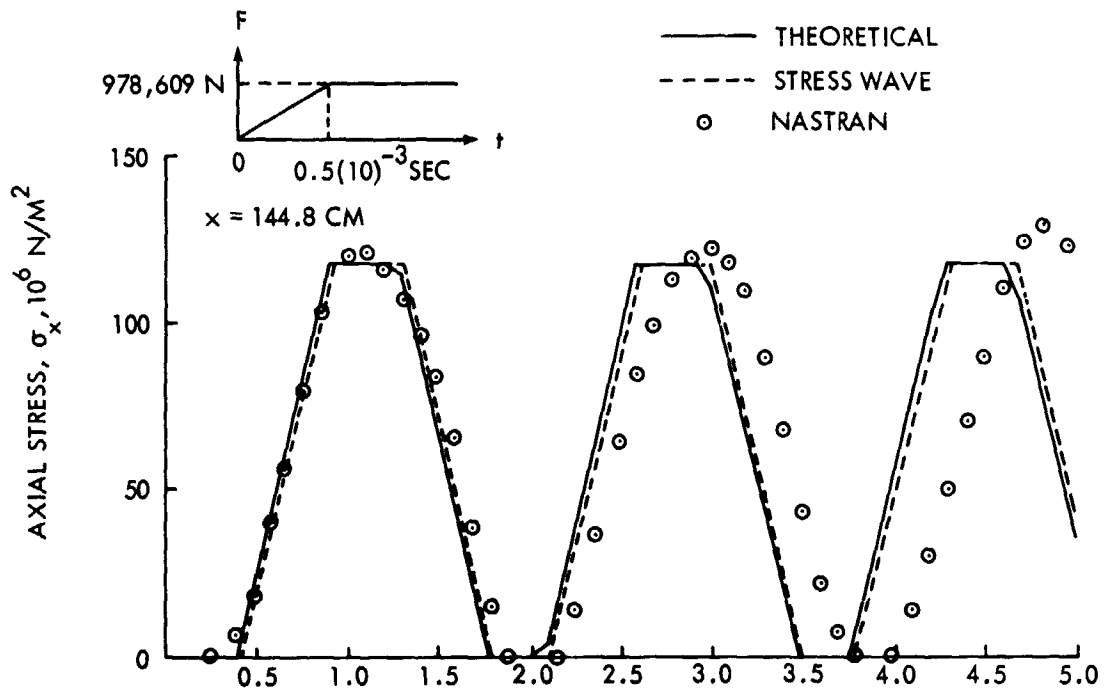


FIGURE 8 AXIAL STRESS

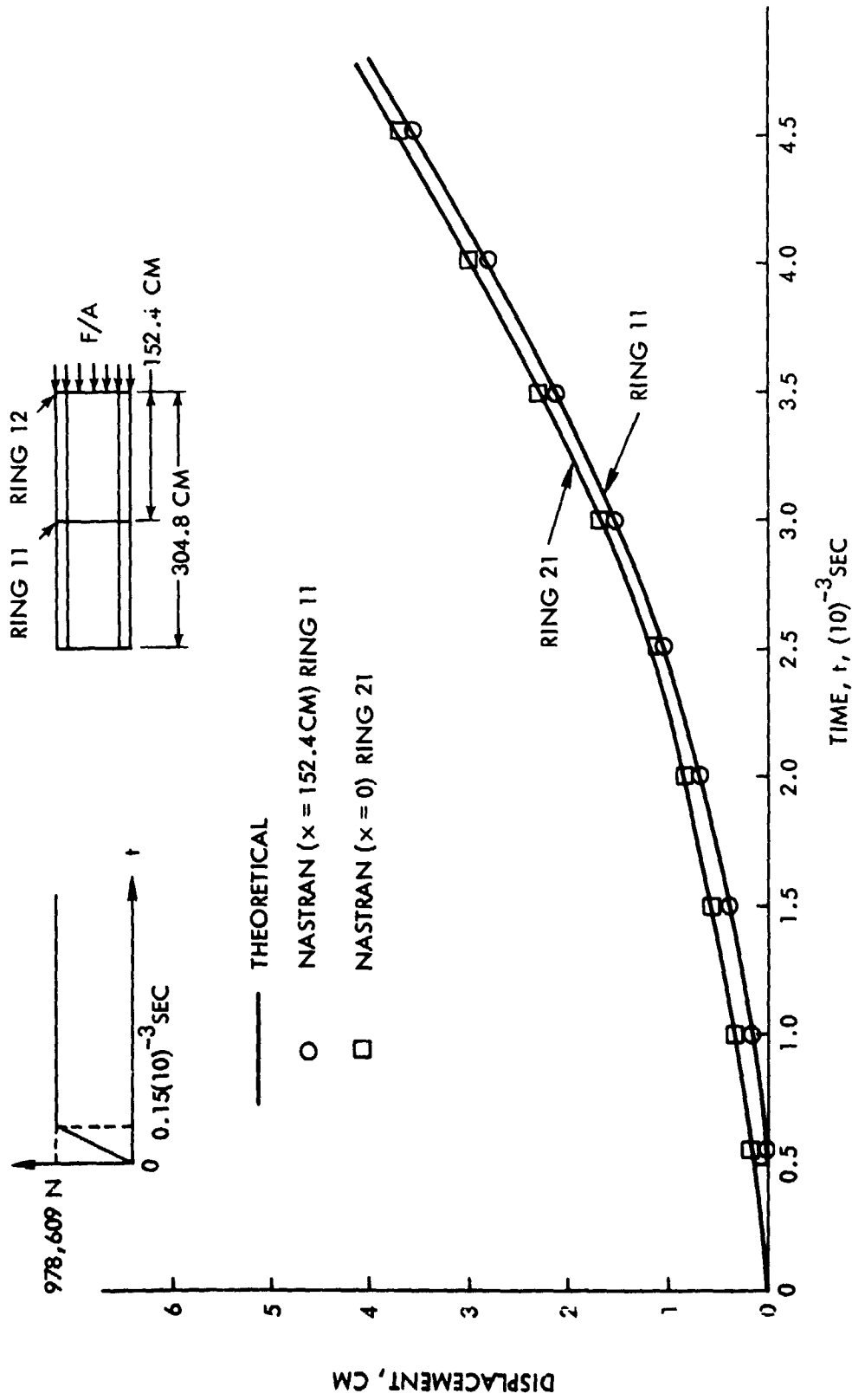


FIGURE 9 AXIAL DISPLACEMENT

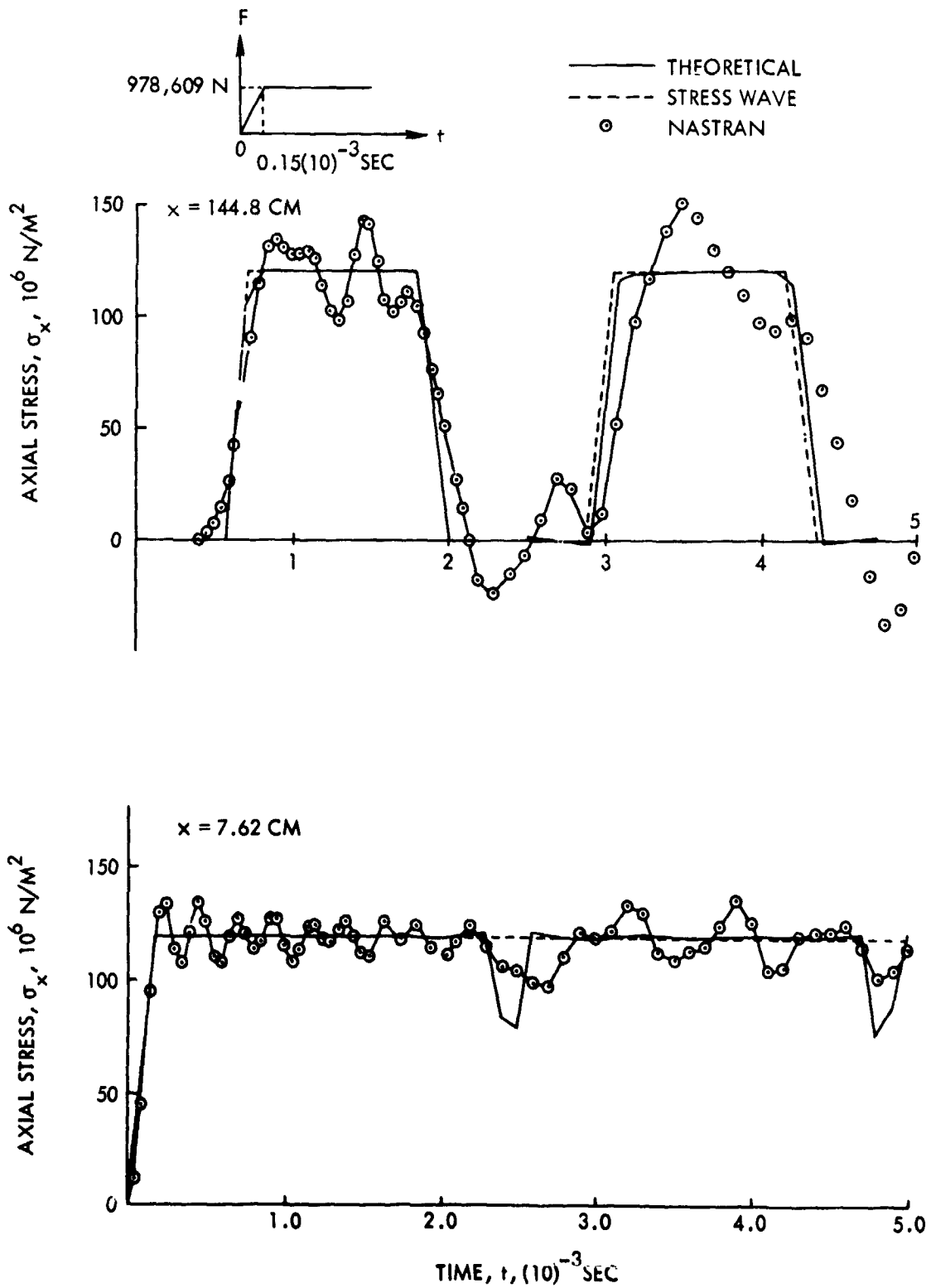


FIGURE 10 AXIAL STRESS

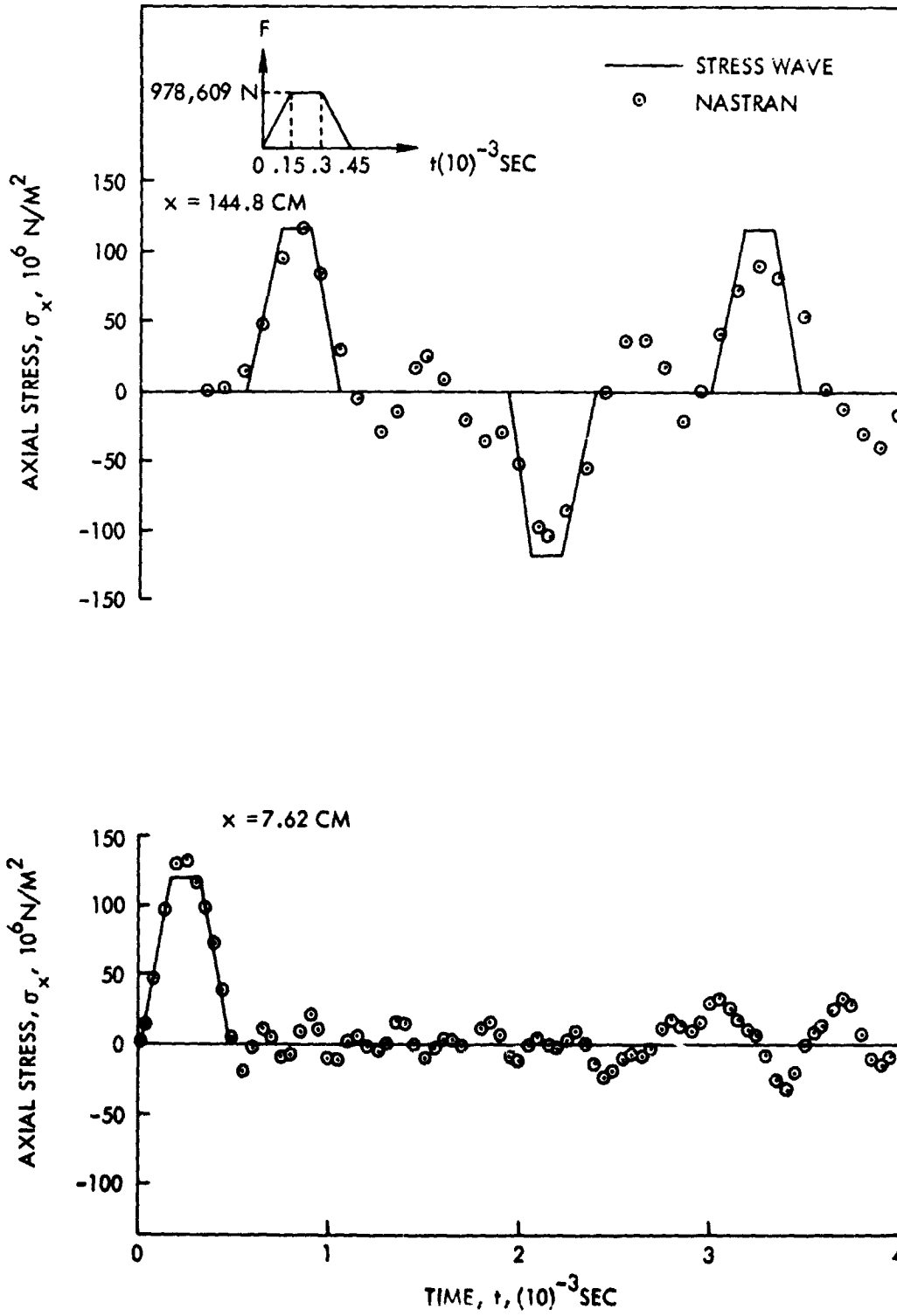


FIGURE 11 AXIAL STRESS

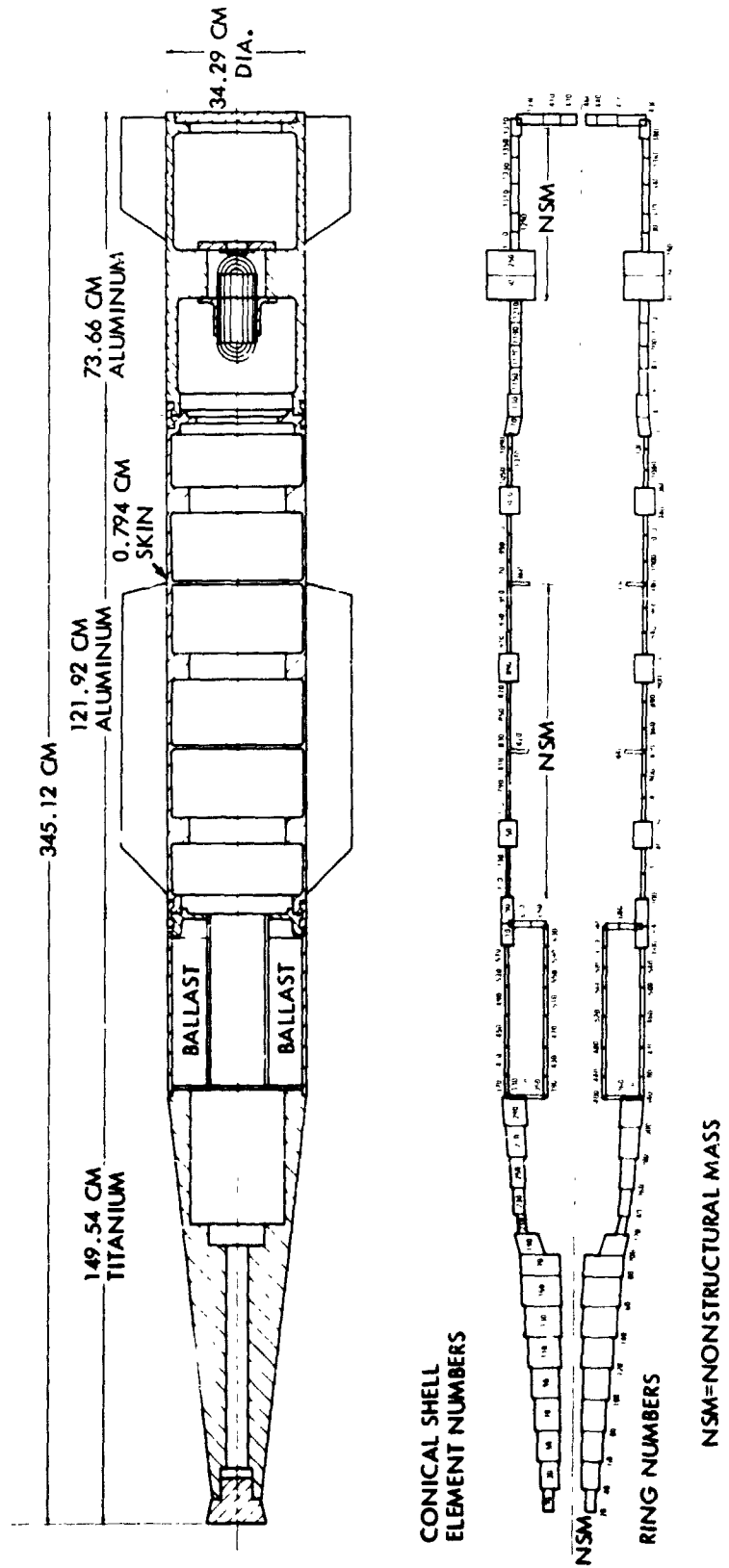


FIG. 12 HYDROBALLISTIC MODEL AND FINITE ELEMENT IDEALIZATION